

RESEARCH ARTICLE

Enriching particles on a bubble through drainage: Measuring and modeling the concentration of microbial particles in a bubble film at rupture

Peter L. L. Walls and James C. Bird

The concentration of microbes and other particulates is frequently enriched in the droplets produced by bursting bubbles. As a bubble rises to the ocean surface, particulates in the bulk liquid can be transported to the sea surface microlayer by attaching to the bubble's interface. When the bubble eventually ruptures, a fraction of these particulates is often ejected into the surroundings in film droplets with a particulate concentration that is higher than in the liquid from which they formed. The precise mechanisms responsible for this enrichment are unclear, yet such enrichment at the ocean surface influences important exchange processes with the atmosphere. Here we provide evidence that drainage, coupled with scavenging, is responsible for the enrichment. By simultaneously recording the drainage and rupture effects with high-speed and standard photography, we directly measured the particulate concentrations in the thin film of a bubble cap at the moment before it ruptures. We observed that the enrichment factor strongly depends on the film thickness at rupture, and developed a physical model, based on scavenging and drainage, that is consistent with our observations. We have also demonstrated that this model is quantitatively consistent with prior observations of film drop enrichment, indicating its potential for a broader range of applications in the study of the sea surface microlayer and related phenomena.

Keywords: scavenging; enrichment; aerosols; film droplets; sea surface microlayer; bubble rupture

Introduction

Covering more than 70% of the Earth's surface, the sea surface microlayer (SML) is critical to a range of transport processes involved in climate change and human health (Després et al., 2012; Cunliffe et al., 2013). For example, bacteria from the SML have been found in the upper atmosphere where they may serve as ice and cloud condensation nuclei, and toxins originating from red tide events are linked to respiratory irritation experienced by coastal residents (Woodcock 1948; Bauer et al., 2003; Kirkpatrick et al., 2004; Després et al., 2012; Cunliffe et al., 2013). In both of these cases, the microscopic particulates involved are transferred by the jet and film droplets formed from the rupture of bubbles entrained by breaking waves (Deane and Stokes, 2002; Lewis and Schwartz, 2004; Grythe et al., 2014; Veron, 2015). Furthermore, it has been observed that the particulate concentration in these droplets is often higher than the concentration in either the bulk water or SML, which amplifies the influence of these particulates (Blanchard and Syzdek, 1970; 1972; Angenent et al., 2005; Aller et al., 2005). Yet, for film drops, it is unclear how large an enrichment

to expect; one previous study reports an enrichment factor between 10 and 20 (Blanchard and Syzdek, 1982), whereas another reports an enrichment factor of over 100 (Wangwongwatana et al., 1990).

Before reaching the ocean surface, entrained air bubbles scavenge particulates from the subsurface water during their rise, ultimately leading to the enrichment that defines the SML (Weber et al., 1983; Aller et al., 2005). As a bubble approaches the surface, it deforms it into a spherical cap (Toba, 1959). The shape of this cap remains constant until the bubble spontaneously ruptures, often fragmenting into film droplets. It is tacitly assumed that the concentration in the enriched film drops is the same as the concentration in the bubble film cap when it is freshly formed. However, because of natural surfactants, the bubble evolves after forming, draining and thinning until rupture (Lhuissier and Villermaux, 2012). Therefore, before rupture, many of the particles initially contained in the bubble cap likely drain back into the bulk liquid. This combination of draining and thinning makes it difficult to assess the impact of each factor on the final enrichment by solely collecting the film droplets produced, as has typically been done in the past (Blanchard and Syzdek, 1982; Wangwongwatana et al., 1990). Instead, our approach is to investigate the film contents immediately *before* rupture. Based on our findings, we have developed a physical

model highlighting the roles of bubble scavenging and drainage in the film as it is rupturing and have demonstrated that our model is quantitatively consistent with the enrichment measurements from films drops collected in earlier studies.

Methods

To better understand the processes leading to an enriched bubble film, we performed a series of single bubble scavenging experiments. The experimental setup used to investigate this process is outlined in **Figure 1**. A cylindrical container was filled with a suspension of common yeast cells, *Saccharomyces cerevisiae*, prepared with tap water at various bulk concentrations C_b ranging from $C_b \approx 10^7$ cells mL^{-1} to $C_b \approx 8 \times 10^7$ cells mL^{-1} . We injected an air bubble of radius $r_b \approx 2.5$ mm (circled in **Figure 1a**) at the bottom of the yeast cell suspension. The newly formed bubble rose a distance $H = 70$ mm and established a spherical cap after reaching the free surface (identified with a dotted rectangle near the top of **Figure 1a**). The drainage and subsequent rupture processes were recorded simultaneously with high-speed and traditional cameras. To ensure that we were able to focus each camera on the bubble and its surface, we overfilled the plastic tube containing the suspension to form a convex meniscus at the top. This technique exploits the natural tendency of the bubble to “self center” in the tube under the influence of gravity.

Before the bubble ruptured, the film thinned and a fraction of the yeast cells initially contained in the bubble cap returned back to the bulk liquid by a combination of gravitational and surface tension forces. We captured this drainage, typically occurring over a time span of seconds, with a standard camera that was fitted with a microscope objective and recorded images at a rate of 30 frames per second. **Figure 1b** shows a segment of a bubble cap as it forms, rests on the interface for nearly two seconds, and then spontaneously pops (see Video S1). Note that the speckles in the images are the individual yeast cells. Additionally, these yeast cells serve as tracers for the flow, revealing that in this video the bubble is draining

at approximately 0.5 mm s^{-1} . These images were taken at a high enough resolution (1.3 microns per pixel) that the number of yeast cells per unit area, N , could be counted immediately before the film ruptured (**Figure 1c**). Because the film was curved, the bubble passed through the focal plane, resulting in a thin region in focus. Cell counts were performed only in this region.

The bubble rupture occurred when a small hole spontaneously initiated and rapidly expanded (see **Figure 1d**). The entire rupturing process, often occurring in less than $t = 2$ ms, was captured with a Photron FASTCAM SA5 high-speed camera at a rate of 60,000 frames per second.

Our choice in using yeast cells rather than other microbial particulates was deliberate. We needed a simple, safe system to make the next series of advances on this topic, though we recognize the potential future value of using marine microorganisms in seawater solution. *Serratia marcescens*, which has been used in the past (Blanchard and Syzdek, 1982), is classified as a human pathogen that requires specialized handling procedures, especially when aerosolized (Yu, 1979). Furthermore, the yeast cells had a measured particle size of $r_p = 3.2 \mu\text{m}$ (standard deviation of $0.4 \mu\text{m}$), which is significantly larger than the previously used bacteria, allowing for easier visualization.

Results and Discussion

As might be expected, the number of yeast cells per area, N , counted in the region of interest at the time of rupture (**Figure 1c**) depended on the bulk concentration C_b , with higher bulk concentrations leading to higher number counts N (**Figure 2a**). In contrast, the film thickness at rupture h appeared to be independent of the bulk yeast concentration C_b over the range of concentrations tested (**Figure 2b**). Here we used the standard technique to measure the film thickness at rupture h by measuring the speed at which the nearly uniform film retracted (Pandit and Davidson, 1990; Lhuissier and Villermaux, 2012; Modini et al., 2013). The surface tension-driven retraction is regulated by inertia and is well approximated by the Taylor-Culick velocity, $\sqrt{2\gamma/\rho h}$, where γ is the surface

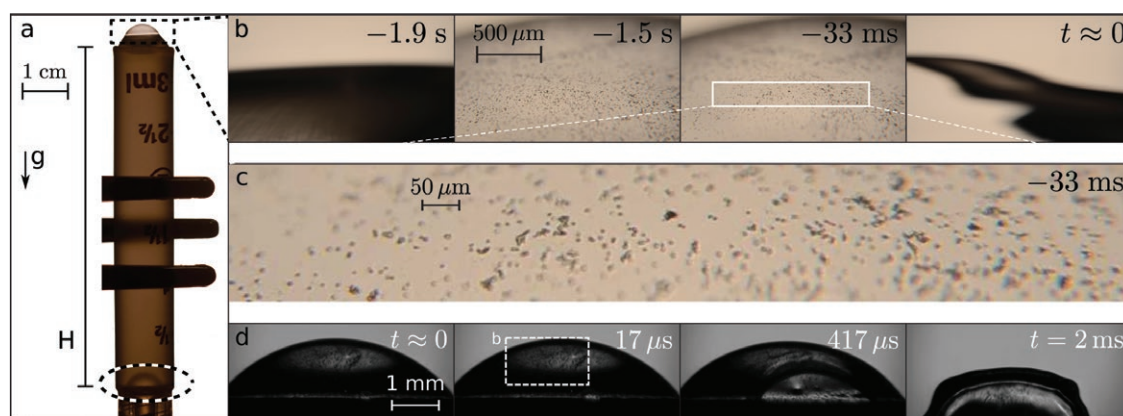


Figure 1: Overview of experimental bubble scavenging procedure. (a) An air bubble is injected at the bottom of a plastic tube and rises through a column of suspended yeast cells of height H forming a spherical bubble cap at the top surface. (b) The bubble’s surface is visualized with a microscope objective mounted on a standard camera. (c) Yeast cells appear as small dark spots on the film. (d) The film thickness at rupture is calculated from the retraction speed recorded with a high-speed camera. DOI: <https://doi.org/10.1525/elementa.230.f1>

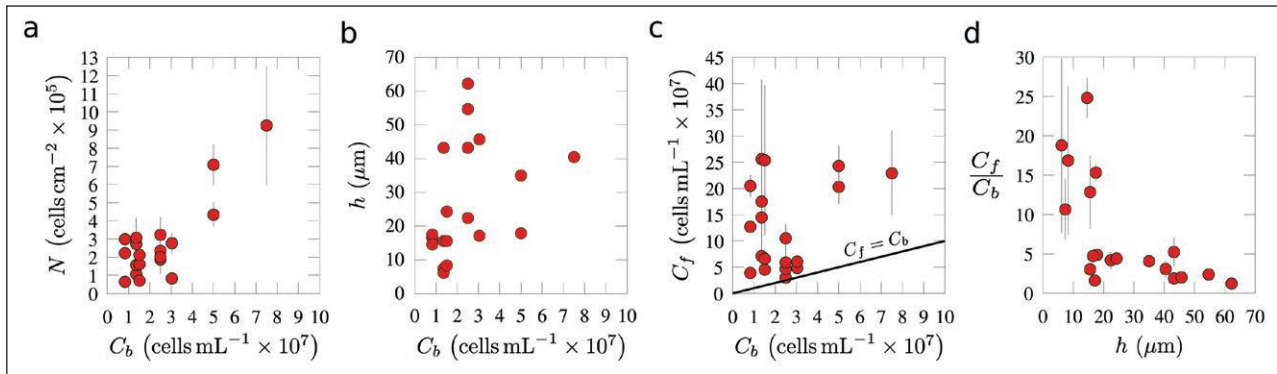


Figure 2: Compilation of results from individual bubble scavenging experiments. (a) The number of yeast cells per area of bubble film at rupture increases with bulk concentration C_b . (b) The thickness at rupture h is independent of C_b . (c) The volumetric concentration of yeast at rupture C_f is also independent of C_b . Data points above the solid line indicate an enriched film ($C_f > C_b$). (d) The enhancement factor of the yeast in the thin film $EF = C_f/C_b$ tends to increase with decreasing film thickness. Error bars indicate a 95% confidence interval of the mean value. Error bars for data points with a confidence interval smaller than the data marker are not shown. DOI: <https://doi.org/10.1525/elementa.230.f2>

tension and ρ is the liquid density (Taylor, 1959; Culick, 1960). The thicknesses at rupture that we measured ranged from $h = 5 \mu\text{m}$ to $h = 60 \mu\text{m}$. These values are larger than what might be expected in particulate-free bubble films (Spiel, 1998; Modini et al., 2013), and we suspect that the presence of particulates may act as nucleation sites that initiate rupture earlier in the drainage process. However, the physics that determine the thickness at which a water bubble spontaneous ruptures is currently unknown (Lhuissier and Villermaux, 2012).

By measuring both the particle surface concentration (N in cells cm^{-2}) and film thickness h at rupture, we were able to calculate the volumetric cell concentration in the thin film $C_f = N/h$, which we report in cells per milliliter. Two noteworthy features become clear when the film concentration at rupture C_f is plotted as a function of the bulk concentration C_b (Figure 2c). First, there is no clear relationship between the two concentrations, and second, the film concentration C_f is categorically larger than the bulk concentration C_b . Specifically, the points in Figure 2c are all above the line denoting equivalence, indicating that the film became enriched.

The ratio of film concentration C_f to the bulk concentration C_b is defined as the enrichment factor EF at rupture. Further insight was gained by plotting this enrichment factor as a function of the rupture film thickness h (Figure 2d). For bubble films that were thick when they ruptured, the film concentration C_f is only slightly larger than the bulk concentration C_b , resulting in an enrichment factor less than ≈ 5 . However, if the bubble film was thinner when it ruptured, the enrichment factor tended to increase. For the thinnest films in our experiments, we measured enrichment factors near 20 (Figure 2d). When thin bubble caps of water drain, it is known that minuscule amounts of indigenous surfactants can rigidify the interface through Marangoni stresses due to surface tension gradients (Scriven and Sternling, 1960). This rigidity of the inner and outer surfaces may lead to the interior of the bubble draining at a faster rate. Indeed,

we saw evidence of this phenomenon in our experiments (see Video S1) where, by taking advantage of our limited visual depth of field, we could see the interior of the film draining downwards while the inner and outer interfaces were, by comparison, stationary. In our experiments, these semi-rigid interfaces were likely caused by the natural surfactants introduced by the yeast.

We can estimate the thickness of the bubble film when it reaches the surface (Figure 1b) by recognizing that the drainage velocity and bubble thickness are coupled through conservation of mass. The film thickness over time decays exponentially if drainage velocity is constant. For the velocity, bubble size, and thickness at rupture, in Figure 1b, this model would predict a thickness of $75 \mu\text{m}$ at $t = -1.9\text{s}$ before rupture. Note that there is evidence that the drainage may be better modeled with a power law (Lhuissier and Villermaux, 2012), although this model in comparison predicts the earlier thickness to be larger than a centimeter. Regardless of the precise drainage dynamics, the bubble thins as it drains until it ruptures at a thickness h that can be measured from the film retraction speed.

To develop a model for the enrichment factor in the spherical cap, we combined the measured values of film thickness at rupture h with the collision efficiency from scavenging theory E_{col} , here defined as the fraction of particles contained in the volume swept out by the bubble that attach to its surface (See Figure 3 for model geometry). Here we use one of the simplest scavenging models, the Sutherland potential flow model $E_{\text{col}} = 3r_p/r_b$ to estimate the number of particles brought to the surface by the rising bubble (Sutherland, 1948). For this model to be appropriate, the scavenged particles should be large enough to ignore diffusive effects ($r_p > 0.1 \mu\text{m}$) and follow the streamlines around the bubble. The flow around the bubble should also be well-approximated as potential flow (Miettinen et al., 2010). Both of these conditions were met by our experiments. Additionally, we assume that any particle colliding with the rising bubble attaches (Figure 3a, b) and remains attached until bursting at

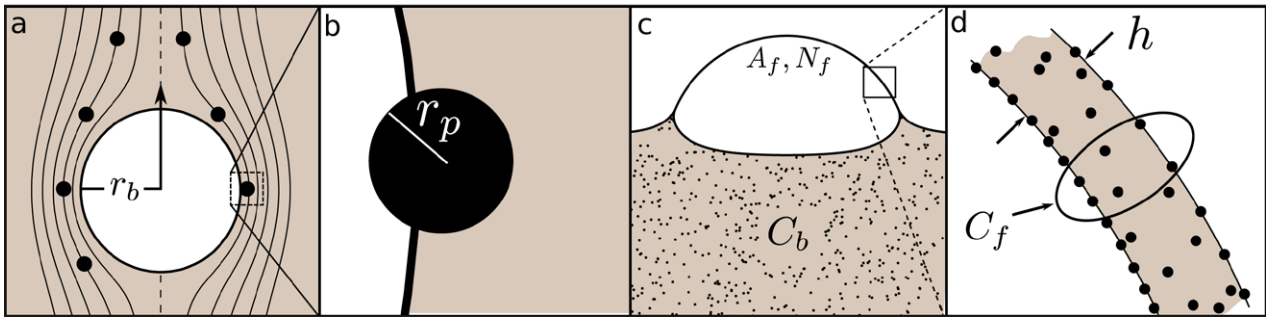


Figure 3: Overview of model geometry. (a) Small particles follow the streamlines as the effects of inertia are negligible. Particles sufficiently far away (left hand side) avoid contacting the bubble. In contrast, the particles close enough for the particle to intercept the bubble (right hand side) will be carried to the surface. (b) Once a particle attaches to the bubble's interface, it forms a three-phase contact line and is brought to the surface. (c) The bubble forms a thin spherical cap of area (A_f) containing a number of particles (N_f) at the liquid surface. (d) The concentration of particulates in the film (C_f) has contributions from the particles scavenged and from particles in the bulk liquid. DOI: <https://doi.org/10.1525/elementa.230.f3>

the free surface. This collision mechanism is commonly referred to as interception, as the particle passes close enough to be “intercepted” by the rising bubble. Although there are more complex collision models that incorporate a large number of parameters, such as particle wettability, density mismatch, and the detaching of particles, our aim is to develop the simplest model that is able to capture the physics of the enrichment process. In addition, the flow conditions may also influence the collision model. For example, in highly turbulent environments, we anticipate the collision efficiency to require modification, typically for larger particles $r_p > 50 \mu\text{m}$, to account for particle velocities that are uncorrelated to the flow conditions immediately surrounding the bubble (Abrahamson, 1975).

For simplicity, our model assumes that the scavenged particles are evenly spread across the bubble surface area. This condition leads to a uniform distribution of particles across the bubble cap area A_f , an assumption that is consistent with our observations during data collection (see **Figure 1b, c**). The total number of particles in the bubble's cap N_f is the sum of two contributions. The first contribution is from the particles scavenged during the bubble's rise that attach to the interface N_{att} (**Figure 3d**) and the second contribution is from the particles contained in the film volume at rupture $A_f h C_b$. The number of particles scavenged by the bubble is determined by multiplying the chosen model for the collision efficiency by the number of particles encountered during the bubble's rise $N_{\text{att}} = E_{\text{col}} \cdot \pi r_b^2 H \cdot C_b = 3\pi r_p r_b H C_b$. Dividing the total number of particles in the film ($N_f = N_{\text{att}} + A_f h C_b$) by the film volume at rupture $A_f h$ yields the film concentration C_f . Introducing a dimensionless grouping of parameters $\Lambda = \frac{h}{H} \frac{r_b}{r_p}$, that we have chosen to scale with the thickness, we finally normalize the film concentration C_f by the original bath concentration C_b , resulting in a prediction for the enrichment factor:

$$\frac{C_f}{C_b} = \frac{3}{4\Lambda} + 1. \quad (1)$$

Re-plotting each of our individual yeast scavenging experiments from **Figure 2** in terms of $\Lambda = \frac{h}{H} \frac{r_b}{r_p}$ and the enrichment factor C_f/C_b results in a reasonable agreement with our model (**Figure 4**). However, like all models there are limitations, and we anticipate instances where our model may not yield good agreement. For example, the biotechnology industry routinely introduces additives, such as the non-ionic surfactant Pluronic® F-68, to prevent cells from attaching to bubbles, as rupturing bubbles are generally agreed to be the largest cause of damage to the cells being grown in production scale bioreactors (Hu et al., 2011). In this example, we would anticipate the film concentration to be approximately equal to the bulk concentration, as the primary method of initially trapping cells in the film has been inhibited, which effectively reduces the collision efficiency to zero. Alternatively, if the density of the scavenged particles were sufficiently large and the bubble long-lived, the particles may sediment, moving independently of the interface, and modify the predicted concentration.

Because we make the assumption that the yeast cells act as passive particles, we would anticipate similar results for inert, non-biological particles. To test this prediction, we ran a separate series of experiments using Polystyrene beads of $r_p = 3 \mu\text{m}$. The same experimental procedure outlined in the Methods section was repeated. Additionally, the Polystyrene beads were suspended in the same water as the yeast after removing the yeast by centrifugation. This step ensured that any natural surfactants present in our original experiments would be maintained. The Polystyrene beads also followed the model reasonably well (**Figure 4**, blue squares). We note that our model tends to underestimate the observed enrichment factors measured in our setup. This underestimation may be due, in part, to the centering of the bubbles with a convex meniscus at the top of our cylindrical container. Specifically, the free surface was not continuously refreshed, leading to the concentration in the upper most layer of the suspension likely being higher than the bulk concentration (Blanchard and Syzdek, 1982).

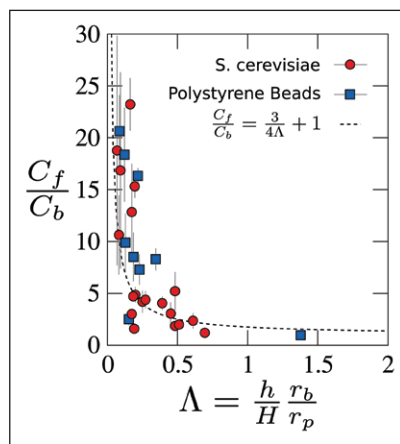


Figure 4: Enrichment factors predicted by our model versus our experimental data. The trend in the enrichment for both sets of data is captured: the thinnest bubbles tend to result in the highest enrichment factors. Our model suggests that the enrichment factor C_f/C_b depends on a single dimensionless grouping $\Lambda = \frac{h}{H} \frac{r_b}{r_p}$, where h is the thickness of the bubble film at rupture, H is the bubble rise height, r_b is the bubble radius, and r_p is the particle radius. Error bars indicate a 95% confidence interval of the mean enrichment factor. Error bars for data points with a confidence interval smaller than the data marker are not shown. DOI: <https://doi.org/10.1525/elementa.230.f4>

We conclude our discussion by comparing our proposed model with two film droplet experiments reported in the literature. Because the thickness at rupture was not measured in either of these studies, we modeled the value of thickness to be equal to the particle size. The first study, by Blanchard and Syzdek (1982), injected air bubbles with radius $r_b = 0.85$ mm that rose a height $H = 19$ mm through a suspension of *Serratia marcescens* bacteria. Because the bacteria are rod-like we use their equivalent radius $r_p = 0.65$ μm (Weber et al., 1983) and assume the bubble ruptured at a thickness $h = 1$ μm , the bacterium's larger dimension. Based on these estimations, we find reasonable agreement between the reported value of enrichment factor $\text{EF} = 18$ and our predicted value of $\text{EF} = 12$.

The second comparison study used latex spheres with particle radius $r_p = 0.28$ μm (Wangwongwatana et al., 1990). Because of the particle size, this example approaches the applicability of our model, specifically that the particles were sufficiently large to ignore diffusive effects. Here the authors injected air bubbles of radius $r_b = 1.29$ mm that rose a height of $H = 600$ mm to the free surface. Although the value of enrichment was not explicitly reported in the study, the authors state that the enrichment factor is well over 100 \times , compared to our expected value of 175.

Finally, we apply the same approximations to our data presented in **Figure 4**. Specifically, we compare the average enrichment factor over the course of our experiments, ignoring the variation between cases. Based on the crude assumption of the bubble rupturing at the thickness of

the particle, $h = 6.4$ μm (the yeast diameter), and accounting for the rise distance in our experiments $H = 70$ mm, our model estimates an approximate overall enrichment factor of 11 versus our measured average EF value of 9. Taken together, these examples illustrate that our model provides a reasonable approximation for the expected enrichment for a wide range of scavenging conditions.

Conclusions

The findings presented in this paper suggest that a combination of both scavenging and drainage concentrate suspended particulates within a bubble cap prior to rupture of the bubble and thus provide a more detailed mechanism of film drop enrichment. Specifically, we provide a framework of the enrichment process as a combination of two steps. First, the bubble transports particles that attach to its interface during its rise to the surface (Weber et al., 1983). Second, after forming a spherical cap at the surface, the bubble drains and thins returning a portion of the scavenged particles back to the bulk. We find that the interior of the bubble cap film drains faster than the inner and outer surfaces. This difference in drainage increases the enrichment factor as the bubble thins. Beyond our bench-scale setup, we compared our model to previous studies and found quantitative agreement between the reported values and our values predicted by our model, supporting the notion that the processes contributing most to particle enrichment occur before the bubble ruptures. Previous studies have demonstrated that bubbles with thinner caps produce a larger number of film drops than thicker caps (Lhuissier and Villermaux, 2012). Additionally, the film drops that these thinner caps produce tend to be smaller and persist longer in the atmosphere (Lewis and Schwartz, 2004; Veron, 2015). Our results suggest that these large number of persistent droplets are also likely to be the most enriched. We anticipate our results may be important to processes involving enriched film drops such as may occur in the sea surface microlayer, with important implications to potential disease or toxin transfer nearshore and climate-related air-sea exchanges on a more global scale.

Supplemental File

The supplemental file for this article can be found as follows:

- **Video S1.** Source video for the images used to construct the times series presented in Figure 1b, c. In the supplemental video, the drainage process is shown twice; first in real time, immediately followed by a version slowed down by 4 \times . Specifically, the bubble appears in frame after rising to the surface, drains, and then disappears as the bubble ruptures. (AVI). DOI: <https://doi.org/10.1525/elementa.230.s1>

Funding information

This work was supported by the National Science Foundation under Grant No. 1351466.

Competing interests

The authors have no competing interests to declare.

Author contributions

All authors contributed equally to this article.

References

- Abrahamson, J** 1975 Collision rates of small particles in a vigorously turbulent fluid. *Chemical Engineering Science* **30**(11): 1371–1379. ISSN 00092509. DOI: [https://doi.org/10.1016/0009-2509\(75\)85067-6](https://doi.org/10.1016/0009-2509(75)85067-6)
- Aller, JY, Kuznetsova, MR, Jahns, CJ and Kemp, PF** 2005 The sea surface microlayer as a source of viral and bacterial enrichment in marine aerosols. *J. Aerosol Sci* **36**(5): 801–812. DOI: <https://doi.org/10.1016/j.jaerosci.2004.10.012>
- Angenent, LT, Kelley, ST, Amand, AS, Pace, NR and Hernandez, MT** 2005 Molecular identification of potential pathogens in water and air of a hospital therapy pool. *Proc. Natl. Acad. Sci* **102**(13): 4860–4865. DOI: <https://doi.org/10.1073/pnas.0501235102>
- Bauer, H, Giebl, H, Hitznerberger, R, Kasper-Giebl, A, Reischl, G, et al.** 2003 Airborne bacteria as cloud condensation nuclei. *J. Geophys. Res* **108**(D21): 1–5. DOI: <https://doi.org/10.1029/2003JD003545>
- Blanchard, DC and Syzdek, L** 1970 Mechanism for the water-to-air transfer and concentration of bacteria. *Science* **170**(3958): 626–628. DOI: <https://doi.org/10.1126/science.170.3958.626>
- Blanchard, DC and Syzdek, LD** 1972 Concentration of bacteria in jet drops from bursting bubbles. *Journal of Geophysical Research* **77**(27): 5087–5099. DOI: <https://doi.org/10.1029/JC077i027p05087>
- Blanchard, DC and Syzdek, LD** 1982 Water-to-air transfer and enrichment of bacteria in drops from bursting bubbles. *Appl Environ Microbiol* **43**(5): 1001–1005.
- Culick, FEC** 1960 Comments on a ruptured soap film. *J Appl Phys* **31**(6): 1128–1129. ISSN 00218979. DOI: <https://doi.org/10.1063/1.1735765>
- Cunliffe, M, Engel, A, Frka, S, Gašparović, B, Guitart, C, et al.** 2013 Sea surface microlayers: A unified physicochemical and biological perspective of the air-ocean interface. *Prog Oceanogr* **109**: 104–116. DOI: <https://doi.org/10.1016/j.pocean.2012.08.004>
- Deane, GB and Stokes, MD** 2002 Scale dependence of bubble creation mechanisms in breaking waves. *Nature* **418**(6900): 839–44. DOI: <https://doi.org/10.1038/nature00967>
- Després, VR, Huffman, JA, Burrows, SM, Hoose, C, Safatov, AS, et al.** 2012 Primary biological aerosol particles in the atmosphere: a review. *Tellus B* **64**. ISSN 1600-0889. DOI: <https://doi.org/10.3402/tellusb.v64i0.15598>
- Grythe, H, Ström, J, Krejci, R, Quinn, P and Stohl, A** 2014 A review of sea-spray aerosol source functions using a large global set of sea salt aerosol concentration measurements. *Atmos Chem Phys* **14**(3): 1277–1297. DOI: <https://doi.org/10.5194/acp-14-1277-2014>
- Hu, W, Berdugo, C and Chalmers, JJ** 2011 The potential of hydrodynamic damage to animal cells of industrial relevance: current understanding. *Cytotechnology* **63**(5): 445–60. DOI: <https://doi.org/10.1007/s10616-011-9368-3>
- Kirkpatrick, B, Fleming, LE, Squicciarini, D, Backer, LC, Clark, R, et al.** 2004 Literature review of Florida red tide: implications for human health effects. *Harmful Algae* **3**(2): 99–115. DOI: <https://doi.org/10.1016/j.hal.2003.08.005>
- Lewis, ER and Schwartz, SE** 2004 *Sea salt aerosol production: mechanisms, methods, measurements and models: a critical review* **152**. Washington, DC: American Geophysical Union. DOI: <https://doi.org/10.1029/GM152>
- Lhuissier, H and Villermaux, E** 2012 Bursting bubble aerosols. *J Fluid Mech* **696**: 5–44. DOI: <https://doi.org/10.1017/jfm.2011.418>
- Miettinen, T, Ralston, J and Fornasiero, D** 2010 The limits of fine particle flotation. *Miner Eng* **23**(5): 420–437. DOI: <https://doi.org/10.1016/j.mineng.2009.12.006>
- Modini, RL, Russell, LM, Deane, GB and Stokes, MD** 2013 Effect of soluble surfactant on bubble persistence and bubble-produced aerosol particles. *J Geophys Res Atmos* **118**(3): 1388–1400. DOI: <https://doi.org/10.1002/jgrd.50186>
- Pandit, AB and Davidson, JF** 1990 Hydrodynamics of the rupture of thin liquid films. *Journal of Fluid Mechanics* **212**: 11. ISSN 0022-1120. DOI: <https://doi.org/10.1017/S0022112090001823>
- Scriven, LE and Sternling, CV** 1960 The Marangoni effects. *Nature* **187**: 186–188. DOI: <https://doi.org/10.1038/187186a0>
- Spiel, DE** 1998 On the births of film drops from bubbles bursting on seawater surfaces. *J Geophys Res Ocean* **103**(C11): 24907–24918. DOI: <https://doi.org/10.1029/98JC02233>
- Sutherland, KL** 1948 Physical chemistry of flotation. XI. kinetics of the flotation process. *J Phys Chem* **52**(5): 394–425. DOI: <https://doi.org/10.1021/j150458a013>
- Taylor, G** 1959 The dynamics of thin sheets of fluid III. Disintegration of fluid sheets. *Proc R Soc London* **253**(1274): 313–321. DOI: <https://doi.org/10.1098/rspa.1959.0196>
- Toba, Y** 1959 Drop production by bursting of air bubbles on the sea surface (II) Theoretical study of the shape of floating bubbles. *J Oceanogr Soc Japan* **15**(3): 121–130.
- Veron, F** 2015 Ocean spray. *Annu Rev Fluid Mech* **47**: 507–538. DOI: <https://doi.org/10.1146/annurev-fluid-010814-014651>
- Wangwongwatana, S, Scarpino, PV, Willeke, K and Baron, PA** 1990 System for characterizing aerosols from bubbling liquids. *Aerosol Sci Technol* **13**(3): 297–307. DOI: <https://doi.org/10.1080/02786829008959446>
- Weber, ME, Blanchard, DC and Syzdek, LD** 1983 The mechanism of scavenging of waterborne

bacteria by a rising bubble. *Limnol Oceanogr* **28**(1): 101–105. DOI: <https://doi.org/10.4319/lo.1983.28.1.0101>

Woodcock, AH 1948 Note concerning human respiratory irritation associated with high concentrations of

plankton and mass mortality of marine organisms. *J Mar Res* **7**(1): 56–62.

Yu, VL 1979 *Serratia marcescens*. *N Engl J Med* **300**(16): 887–893. DOI: <https://doi.org/10.1056/NEJM197904193001604>

How to cite this article: Walls, PLL and Bird, JC 2017 Enriching particles on a bubble through drainage: Measuring and modeling the concentration of microbial particles in a bubble film at rupture. *Elem Sci Anth*, 5: 34, DOI: <https://doi.org/10.1525/elementa.230>

Domain Editor-in-Chief: Jody W. Deming, University of Washington, US

Knowledge Domain: Ocean Science

Part of an *Elementa* Special Feature: The Sea Surface Microlayer – Linking the Ocean and Atmosphere

Submitted: 28 February 2017

Accepted: 09 June 2017

Published: 30 June 2017

Copyright: © 2017 The Author(s). This is an open-access article distributed under the terms of the Creative Commons Attribution 4.0 International License (CC-BY 4.0), which permits unrestricted use, distribution, and reproduction in any medium, provided the original author and source are credited. See <http://creativecommons.org/licenses/by/4.0/>.



Elem Sci Anth is a peer-reviewed open access journal published by University of California Press.

OPEN ACCESS 